SUPPLEMENTARY INFORMATION

On the 'centre of gravity' method for measuring the composition of magnetite/maghemite mixtures, or the stoichiometry of magnetite-maghemite solid solutions, via ^{57}Fe Mössbauer spectroscopy

Jeppe Fock[1], Lara K. Bogart[2], David González-Alonso[3], Jose I. Espeso[3], Mikkel F. Hansen[1], Miriam Varon[4], Cathrine Frandsen[4] and Quentin A. Pankhurst[2]

[1] Department of Micro- and Nanotechnology, DTU Nanotech, Building 345B, Technical University of Denmark, DK-2800 Kongens Lyngby, Denmark
[2] Healthcare Biomagnetics Laboratory, University College London, 21 Albemarle Street, London W1S 4BS, UK
[3] Departamento CITIMAC, Universidad de Cantabria, 39005 Santander, Spain
[4] Department of Physics, DTU Physics, Building 307, Technical University of Denmark, DK-2800 Kongens Lyngby, Denmark

S1. Algebraic formulae relating α to *x* in mixtures and solid solutions, and α to *w* in mixtures

S1(a). Algebraic formulae relating α to *x* in mixtures

Definitions:

$$\alpha = \frac{\text{the number of Fe atoms present in the form of magnetite } (\mathrm{Fe_3O_4})}{\text{the total number of Fe atoms in the mixture}}\,, \qquad \text{(S1.1)}$$

$$x = \frac{\text{the number of Fe}^{2+}\text{atoms present in the mixture}}{\text{the number of Fe}^{3+}\text{atoms present in the mixture}} = \frac{n_{\mathrm{Fe^{2+}}}}{n_{\mathrm{Fe^{3+}}}}\,. \qquad \text{(S1.2)}$$

We consider a mixture comprising $n_{\mathrm{Fe_3O_4}}$ moles of magnetite, Fe_3O_4, where two of the three Fe atoms are in the 3+ charge state, and one is in the 2+ charge state; and $n_{\gamma-\mathrm{Fe_2O_3}}$ moles of maghemite, γ-Fe_2O_3, where both Fe atoms are in the 3+ charge state. To express α in terms of x, we start with

$$\alpha = \frac{3n_{\mathrm{Fe_3O_4}}}{3n_{\mathrm{Fe_3O_4}}+2n_{\gamma-\mathrm{Fe_2O_3}}}\,, \quad \text{and} \quad x = \frac{n_{\mathrm{Fe_3O_4}}}{2n_{\mathrm{Fe_3O_4}}+2n_{\gamma-\mathrm{Fe_2O_3}}}\,. \qquad \text{(S1.3)}$$

Then

$$2n_{\gamma-\mathrm{Fe_2O_3}} = \frac{n_{\mathrm{Fe_3O_4}}}{x} - 2n_{\mathrm{Fe_3O_4}}\,, \qquad \text{(S1.4)}$$

and

$$\alpha = \frac{3n_{\mathrm{Fe_3O_4}}}{3n_{\mathrm{Fe_3O_4}} + \frac{n_{\mathrm{Fe_3O_4}}}{x} - 2n_{\mathrm{Fe_3O_4}}} = \frac{3}{1+\frac{1}{x}}\,. \qquad \text{(S1.5)}$$

Hence

$$\boxed{\alpha = \frac{3x}{1+x} \quad \text{and} \quad x = \frac{\alpha}{3-\alpha}\,. \qquad \text{(S1.6)}}$$

S1(b). Algebraic formulae relating α to *x* in a solid solution.

The values of α and x are defined in Eqs. (S1.1) and (S1.2). We consider a solid solution (also known as a non-stoichiometric or partially oxidized magnetite, or an intermediate phase) defined as

$$\mathrm{Fe^{3+}}[\{\mathrm{Fe}^{2+}_a\mathrm{Fe}^{3+}_a\}\mathrm{Fe}^{3+}_b\square_{2-2a-b}]\mathrm{O_4}\;\;,$$

where charge balance dictates that $5a + 3b = 5$.

We can rewrite this formula as if the material was a superposition of a magnetite phase and a maghemite phase, as

$$a\mathrm{Fe^{3+}}[\mathrm{Fe^{2+}Fe^{3+}}]\mathrm{O_4} \;+\; (1-a)\mathrm{Fe^{3+}}\left[\mathrm{Fe}^{3+}_{5/3}\square_{1/3}\right]\mathrm{O_4}.$$

To express α in terms of x, we first express both in terms of a as

$$\alpha = \frac{3a}{3a+\frac{8}{3}(1-a)} = \frac{9a}{8+a}\,, \quad \text{and} \quad x = \frac{a}{\frac{8}{3}-\frac{2}{3}a} = \frac{3a}{8-2a}\,. \qquad \text{(S1.7)}$$

Rearranging and equating these, we obtain as before

$$\boxed{\alpha = \frac{3x}{1+x} \quad \text{and} \quad x = \frac{\alpha}{3-\alpha}\,. \qquad \text{(S1.8)}}$$

S1(c). Algebraic formulae relating *x* to *a* and *b* in a solid solution

In a solid solution, the formula unit is written as

$$\mathrm{Fe^{3+}[\{Fe_{a}^{2+}Fe_{a}^{3+}\}Fe_{b}^{3+}\square_{2-2a-b}]O_4} \ ,$$

where charge balance dictates that 5*a* + 3*b* = 5. The *a* and *b* occupancy parameters may be derived from *x* as

$$x = \frac{n_{\mathrm{Fe^{2+}}}}{n_{\mathrm{Fe^{3+}}}} = \frac{a}{1+a+b} \quad \text{and} \quad b = \frac{5-5a}{3} \ , \tag{S1.9}$$

which upon rearranging gives

$$\boxed{a = \frac{8x}{3+2x} \qquad \text{and} \qquad b = \frac{5-10x}{3+2x} \quad .} \tag{S1.10}$$

S1(d). Algebraic formulae relating α to ϵ

The parameter ϵ describes the oxidation from magnetite ($\epsilon = 0$) to maghemite ($\epsilon = \frac{1}{9}$) according to:

$$\mathrm{Fe_{3(1-\epsilon)}O_4} \tag{S1.11}$$

We can relate ϵ to x using Eq. (S1.10) as

$$\begin{aligned} 3(1-\epsilon) &= 1 + 2a + b \\ &= 1 + 2\frac{8x}{3\ +\ 2x} + \frac{5\ -\ 10x}{3\ +\ 2x} \\ \epsilon &= \frac{1-2x}{9\ +\ 6x} \end{aligned} \tag{S1.12}$$

Further

$$x = \frac{(1-9\epsilon)}{(2+6\epsilon)} \tag{S1.13}$$

Relating to α using Eq. (S1.8) gives

$$\alpha = \frac{(1-9\epsilon)}{(1-\epsilon)} \tag{S1.14}$$

S1(e). Algebraic formulae relating α to *w* in mixtures.

Definitions:

$$\alpha = \frac{\text{the number of Fe atoms present in the form of magnetite}}{\text{the total number of Fe atoms in the mixture}} = \frac{3n_{\mathrm{Fe_3O_4}}}{3n_{\mathrm{Fe_3O_4}} + 2n_{\gamma-\mathrm{Fe_2O_3}}} \ , \tag{S1.15}$$

$$\begin{aligned} w &= \frac{\text{the mass of magnetite present in the mixture}}{\text{the total mass of magnetite and maghemite present in the mixture}} \\ &= \frac{n_{\mathrm{Fe_3O_4}} M_{\mathrm{Fe_3O_4}}}{n_{\mathrm{Fe_3O_4}} M_{\mathrm{Fe_3O_4}} + n_{\gamma-\mathrm{Fe_2O_3}} M_{\gamma-\mathrm{Fe_2O_3}}} \end{aligned} \tag{S1.16}$$

where n and M are the number of moles and the molecular weights, respectively, of the magnetite, Fe_3O_4, and maghemite, γ-Fe_2O_3, phases.

To express α in terms of w, we first solve both equations for $n_{\gamma-\mathrm{Fe_2O_3}}$

$$n_{\gamma-\mathrm{Fe_2O_3}} = n_{\mathrm{Fe_3O_4}} \frac{3-3\alpha}{2\alpha} \quad \text{and} \quad n_{\gamma-\mathrm{Fe_2O_3}} = n_{\mathrm{Fe_3O_4}} \frac{M_{\mathrm{Fe_3O_4}}(1-w)}{M_{\gamma-\mathrm{Fe_2O_3}} w}. \tag{S1.17}$$

Rearranging and equating these, we obtain

$$\alpha = \frac{3M_{\gamma-\mathrm{Fe_2O_3}} w}{2M_{\mathrm{Fe_3O_4}} + \left(3M_{\gamma-\mathrm{Fe_2O_3}} - 2M_{\mathrm{Fe_3O_4}}\right) w}, \tag{S1.18}$$

$$\text{and} \qquad w = \frac{2M_{\mathrm{Fe_3O_4}} \alpha}{3M_{\gamma-\mathrm{Fe_2O_3}} + \left(2M_{\mathrm{Fe_3O_4}} - 3M_{\gamma-\mathrm{Fe_2O_3}}\right) \alpha} \quad . \tag{S1.19}$$

Inserting $M_{\mathrm{Fe_3O_4}}$= 231.5326 g/mol and $M_{\gamma-\mathrm{Fe_2O_3}}$ = 159.6882 g/mol, we obtain the approximate expressions

$$\boxed{\alpha \approx \frac{29.94\, w}{28.94 + w} \qquad \text{and} \qquad w \approx \frac{28.94\, \alpha}{29.94 - \alpha} \ .} \tag{S1.20}$$

S2. Notes on the 'centre of gravity' Mössbauer fitting methodology

S2(a). Pairwise relative areas constraint in subcomponent sextets

In Section 3 a comment is made regarding the need to constrain the pairwise relative areas of any subcomponent sextets used in the analysis. The text in the paper reads:

Alternatively, one can consider the counter-example in which the pairwise relative areas in the component sextets are different, e.g. 3 : x : y. A quadrupole shift ε_i *would shift the outermost pair of lines by* $+\varepsilon_i$ *towards a more positive velocity, whereas the other four lines would be shifted by -*ε_i *towards a more negative velocity. As such, the isomer shift of the sextet as a whole would no longer be* δ_i*, but would be* $\delta_i + \frac{(3-x-y)}{(3+x+y)}\,\varepsilon_i$*, and the centre of gravity methodology would have fallen down.*

Here we are simply applying equation (11), i.e. $\bar{\delta} = \sum_j A_j\, \delta_j \,/\, \sum_j A_j$, to the case of a given subcomponent sextet. The six lines in the sextet have areas 3, x, y, y, x, and 3, respectively, so that $\sum_j A_j = A_{\text{total}}$ = 6 + 2x + 2y, and the isomer shift is given by:

$$\delta_i + \frac{3}{A_{\text{total}}}\,\varepsilon_i - \frac{x}{A_{\text{total}}}\,\varepsilon_i - \frac{y}{A_{\text{total}}}\,\varepsilon_i - \frac{y}{A_{\text{total}}}\,\varepsilon_i - \frac{x}{A_{\text{total}}}\,\varepsilon_i + \frac{3}{A_{\text{total}}}\,\varepsilon_i \qquad \text{(S2.1)}$$

where we add the contributions from each of the six lines. This reduces directly to the expression:

$$\delta_i + \frac{(3-x-y)}{(3+x+y)}\,\varepsilon_i \qquad \text{(S2.2)}$$

as cited in the text.

S2(b). Lorentzian and Voigtian line profiles

Spectra were fitted using either Lorentzian line shapes or Voigtian line shapes. A Lorentzian line (centred at v = 0) is given by

$$L(v,\gamma) = \frac{\gamma}{\pi(v^2+\gamma^2)}, \qquad \text{(S2.3)}$$

and it thus has half width at half maximum (HWHM) = γ and full width at half maximum (FWHM) = 2γ. The Voigtian line shape $V(v)$ is a convolution of the Lorentzian line shape with a Gaussian, i.e.

$$V(v,\sigma,\gamma) = \int_{-\infty}^{+\infty} G(v',\sigma)\, L(v-v',\gamma)\, \mathrm{d}v', \qquad \text{(S2.4)}$$

with the Gaussian line shape

$$G(v,\sigma) = \frac{1}{\sigma\sqrt{2\pi}} \exp\left(-\frac{v^2}{2\sigma^2}\right). \qquad \text{(S2.5)}$$

The Voigtian line shape can be used to account for a distribution in parameters, such as the hyperfine field splitting (where the ratios between the values of σ for lines 1, 2 and 3 are then pre-defined values).

S3. Standard samples.

S3(a). Standard samples – photographs.

S3(b). Standard samples – DTU100 purity determined from Verwey transition data.

The Verwey transition temperature has been found to be sensitive to the stoichiometry of magnetite by Shepherd *et al.* [1], as illustrated in the following figure adapted from data presented in that paper.

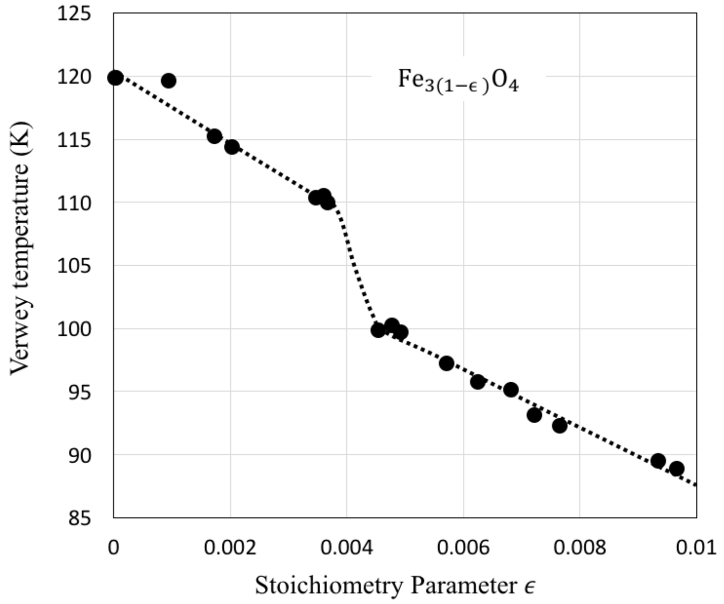

The observed Verwey temperature for DTU100 was centered at ca. 107 K, but was rather broad, starting at ca. 95 K and completing at ca. 115 K. Using these figures we estimate from the Shepherd results that the parameter ϵ in $Fe_{3(1-\epsilon)}O_4$ has an value ϵ = 0.004 ± 0.002.

Using Eq. (S1.14), $\alpha = \frac{(1-9\epsilon)}{(1-\epsilon)}$, this corresponds to $\boldsymbol{\alpha}$ **= 0.968 ± 0.016**.

References

[1] Shepherd J P, Koenitzer J W, Aragón R, Spal/ek J and Honig J M 1991 Heat capacity and entropy of nonstoichiometric magnetite $Fe_{3(1-\delta)}O_4$: the thermodynamic nature of the Verwey transition Phys. Rev. B 43 8461–71

S3(c). Standard samples – DTU100 purity determined from Mössbauer data.

For well resolved Mössbauer spectra with sharps lines the magnetite purity can be determined from the area ratio, r_{AB} , of the A (octahedral) and B (tetrahedral) sites corresponding to the inner and outer sextets respectively [2]. From eq. 4 in [1] we have

$$r_{\mathrm{AB}} = \frac{f_{\mathrm{A}}}{f_{\mathrm{B}}}\frac{n_A}{n_B} = \frac{f_{\mathrm{A}}}{f_{\mathrm{B}}}\frac{2a}{(1+b)} \tag{S3.1}$$

Where $\frac{f_A}{f_B}$ is the ratio between the recoil free fractions of the A and B sites.

Applying the requirement of charge neutrality, we have $5a + 3b = 5$. Thus:

$$r_{\mathrm{AB}} = \frac{f_{\mathrm{A}}}{f_{\mathrm{B}}}\frac{(2-\frac{6}{5}b)}{(1+b)}$$

$$b = \frac{(10 - 5\frac{f_{\mathrm{B}}}{f_{\mathrm{A}}}r_{\mathrm{AB}})}{(6 + 5\frac{f_{\mathrm{B}}}{f_{\mathrm{A}}}r_{\mathrm{AB}})} \quad \text{and} \quad a = \frac{8\frac{f_{\mathrm{B}}}{f_{\mathrm{A}}}r_{\mathrm{AB}}}{(6 + 5\frac{f_{\mathrm{B}}}{f_{\mathrm{A}}}r_{\mathrm{AB}})} \,. \tag{S3.2}$$

Now we can express α in terms of r_{AB}:

$$\alpha = \frac{9a}{8 + a} = \frac{3\frac{f_{\mathrm{B}}}{f_{\mathrm{A}}}r_{\mathrm{AB}}}{2\left(1 + \frac{f_{\mathrm{B}}}{f_{\mathrm{A}}}r_{\mathrm{AB}}\right)} \tag{S3.3}$$

$$\alpha = \frac{3}{2}\frac{1.05\, r_{\mathrm{AB}}}{(1 + 1.05\, r_{\mathrm{AB}})} \tag{S3.4}$$

The fitted area ratio r_{AB} is 1.76 ± 0.05 for the UCL data, where we definine site A as corresponding to those sextets having an isomer shift above 0.6 mm/s and site B as those sextets which have an isomer shift below 0.6 mm/s. From this we estimate that **α = 0.973 ± 0.010**.

References

[2] da Costa G M, Blanco-Andujar C, De Grave E and Pankhurst Q A 2014 Magnetic nanoparticles for in vivo use: a critical assessment of their composition. J. Phys. Chem. B 118 11738–46.

S4. Calculation of knee of $M(H)$ curves of DTU100 and DTU0 samples at room temperature

Although it is not often reported, the ‘knee’ of the magnetization curve is a well-defined and useful parameter containing information about the magnetic anisotropy and domain structure of a magnetic material. However, it is a parameter that can be problematic as it is often obtained by subjective scrutiny of a magnetization curve, rather than by applying a standard procedure.

The following is the procedure that we have applied to measure H_{knee} for the DTU100 magnetite and DTU0 maghemite samples:

1. First, the anhysteretic part of the first quadrant of the $M(H)$ curve was obtained by averaging the upper and lower branches of the measured hysteresis curves.

2. Next, the magnetization M was converted from the measured mass magnetization (unit: Am^2/kg) into the corresponding volumetric magnetization (unit: kA/m) by dividing with the respective densities of magnetite ($\rho_{\mathrm{Fe_3O_4}}$ = 5.15 g/cm^3) and maghemite ($\rho_{\gamma-\mathrm{Fe_2O_3}}$= 4.9 g/cm^3).
   This yielded the anhysteretic magnetisation curves (shown alongside the as-measured hysteretic curves) for DTU100 magnetite:

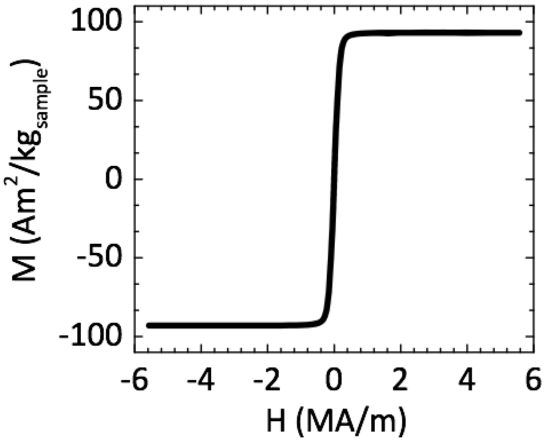

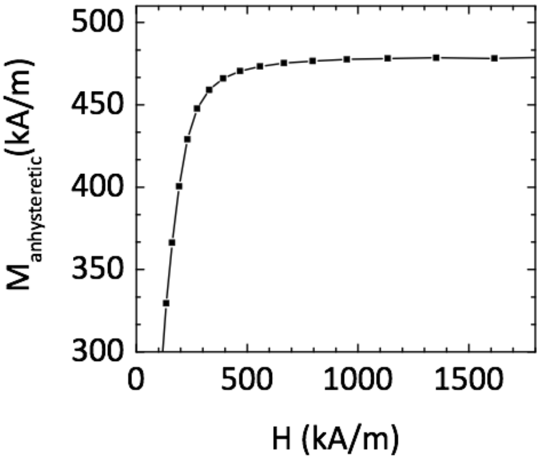

and for DTU0 maghemite:

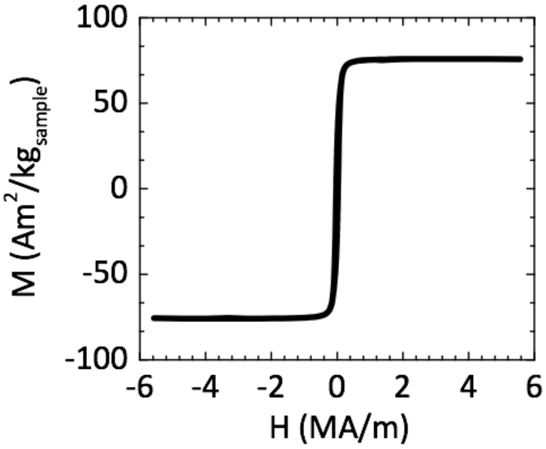

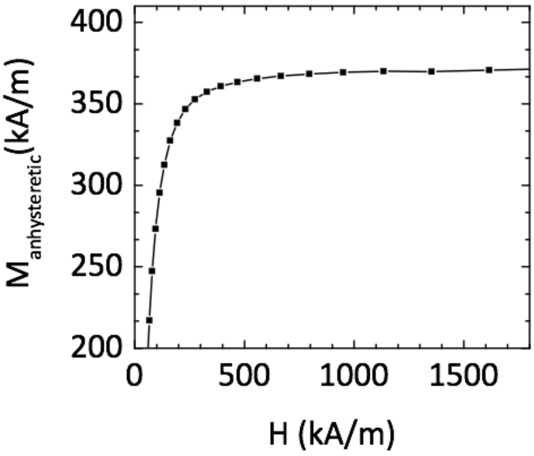

3. The curvature function $\kappa(H)$ was calculated numerically according to

$$\kappa = \frac{|\mathrm{d}^2 M/\mathrm{d}\,H^2|}{[1 + \ (\mathrm{d}M/\mathrm{d}H)^2]^{\ 3/2}} \tag{S4.1}$$

yielding the curves shown as insets in the figure:

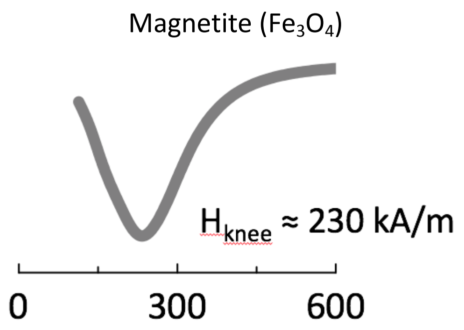

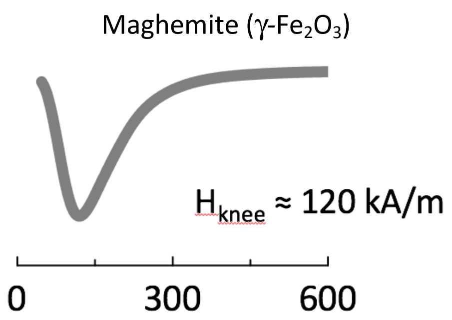

S5. Fits to Mössbauer data of the DTU100 magnetite and DTU0 maghemite samples

As described in Section S2(b), spectra were fitted using either Lorentzian line shapes or Voigtian line shapes. The Voigtian line shape can be used to account for a distribution in parameters, such as the hyperfine field splitting (where the ratios between the values of σ for lines 1, 2 and 3 are then pre-defined values). In some cases more than one hyperfine field distribution has been allowed in the fit. In these cases, the values of the isomer quadrupole shifts were identical for the two components.

For the DTU100 magnetite:

Lorentzian line fit						
a = 100 %	**MSE = 5.9**	**$\bar{\delta}$ = 0.527 ± 0.002 mm/s**				
δ [mm/s]	ε [mm/s]	$\mu_0 H_{\mathrm{hf}}$ [T]	$2\gamma_{1,6}$ [mm/s]	$2\gamma_{2,5}$ [mm/s]	$2\gamma_{3,4}$ [mm/s]	Area [%]
0.265 ± 0.000	-0.01 ± 0.00	49.11 ± 0.00	0.29 ± 0.00	0.25 ± 0.00	0.23 ± 0.00	36.17 ± 0.13
0.665 ± 0.001	-0.03 ± 0.00	46.10 ± 0.00	0.34 ± 0.00	0.27 ± 0.00	0.24 ± 0.00	46.18 ± 0.96
0.702 ± 0.001	0.12 ± 0.00	46.09 ± 0.01	0.34 ± 0.01	0.31 ± 0.01	0.20 ± 0.01	17.65 ± 0.95

For the DTU0 maghemite:

Voigtian line fit						
a = 0 %	**MSE = 3.9**	**$\bar{\delta}$ = 0.321 ± 0.004 mm/s**		**Lorentzian: γ = 0.174 mm/s**		
δ [mm/s]	ε [mm/s]	$\mu_0 H_{\mathrm{hf}}$ [T]	$2\sigma_{1,6}$ [mm/s]	$2\sigma_{2,5}$ [mm/s]	$2\sigma_{3,4}$ [mm/s]	Area [%]
0.271 ± 0.002	0.08 ± 0.00	50.69 ± 0.08	0.02 ± 0.13	0.01 ± 0.07	0.00 ± 0.02	13.98 ± 1.97
		49.42 ± 0.06	0.06 ± 0.04	0.03 ± 0.03	0.01 ± 0.01	18.91 ± 2.08
0.346 ± 0.001	-0.05 ± 0.00	49.36 ± 0.01	0.40 ± 0.00	0.23 ± 0.00	0.06 ± 0.00	51.83 ± 0.76
		36.46 ± 0.61	4.94 ± 0.15	2.86 ± 0.09	0.78 ± 0.02	15.28 ± 0.64

S6. Determination of the α parameter for the mixtures used in the Mössbauer experiments

The weight percentage is calculated using:

$$w = \frac{\alpha_2\, m_{\mathrm{Fe_3O_4}}}{m_{\mathrm{Fe_3O_4}} + m_{\gamma-\mathrm{Fe_2O_3}}} \tag{S6.1}$$

with the masses given in the table below, and α_2 = 0.97 is defined as the established α value of the DTU100 magnetite. Subsequently α is calculated using Eq. (S1.18). The uncertainties in the determination of masses are estimated to dm =0.1 mg, thus the uncertainty in w is

$$\mathrm{d}w = \frac{\sqrt{m^2_{\mathrm{Fe_3O_4}} + m^2_{\gamma-\mathrm{Fe_2O_3}}}}{(m_{\mathrm{Fe_3O_4}} + m_{\gamma-\mathrm{Fe_2O_3}})^2}\,\mathrm{d}m. \tag{S6.1}$$

The corresponding uncertainty on α is

$$\mathrm{d}\alpha = \frac{k_1 k_2}{(w + k_2)^2}\mathrm{d}w \tag{S6.3}$$

with

$$\mathrm{k}_1 = \frac{3M_{\gamma-\mathrm{Fe_2O_3}}}{3M_{\gamma-\mathrm{Fe_2O_3}} - 2M_{\mathrm{Fe_3O_4}}} \simeq 29.94 \quad \text{and} \quad k_2 = \frac{2M_{\mathrm{Fe_3O_4}}}{3M_{\gamma-\mathrm{Fe_2O_3}} - 2M_{\mathrm{Fe_3O_4}}} \simeq 28.94. \tag{S6.4}$$

Sample	**1**	**2**	**3**	**4**	**5**	**6**	**7**	**8**	**9**
$\boldsymbol{m_{\gamma-\mathrm{Fe_2O_3}}}$ **[mg]**	378.1	356.8	278.7	243.5	212.4	194.8	270.5	244.9	91.8
$\boldsymbol{m_{\mathrm{Fe_3O_4}}}$**[mg]**	90.5	43.7	132.4	168.2	239.7	288.1	622.9	991.5	853.2
$\frac{w}{\alpha_2}$ [%]	19.31	10.91	32.21	40.85	53.02	59.66	69.72	80.19	90.29
$\frac{\alpha}{\alpha_2}$ [%]	19.85	11.25	32.95	41.68	53.86	60.48	70.43	80.73	90.58
$\frac{\mathrm{d}w}{\alpha_2}$ [%]	0.02	0.02	0.02	0.02	0.02	0.01	0.01	0.01	0.01
$\frac{\mathrm{d}\alpha}{\alpha_2}$ [%]	0.02	0.02	0.02	0.02	0.02	0.01	0.01	0.01	0.01

S7. Representative Mössbauer fitting parameters of magnetite/maghemite mixtures

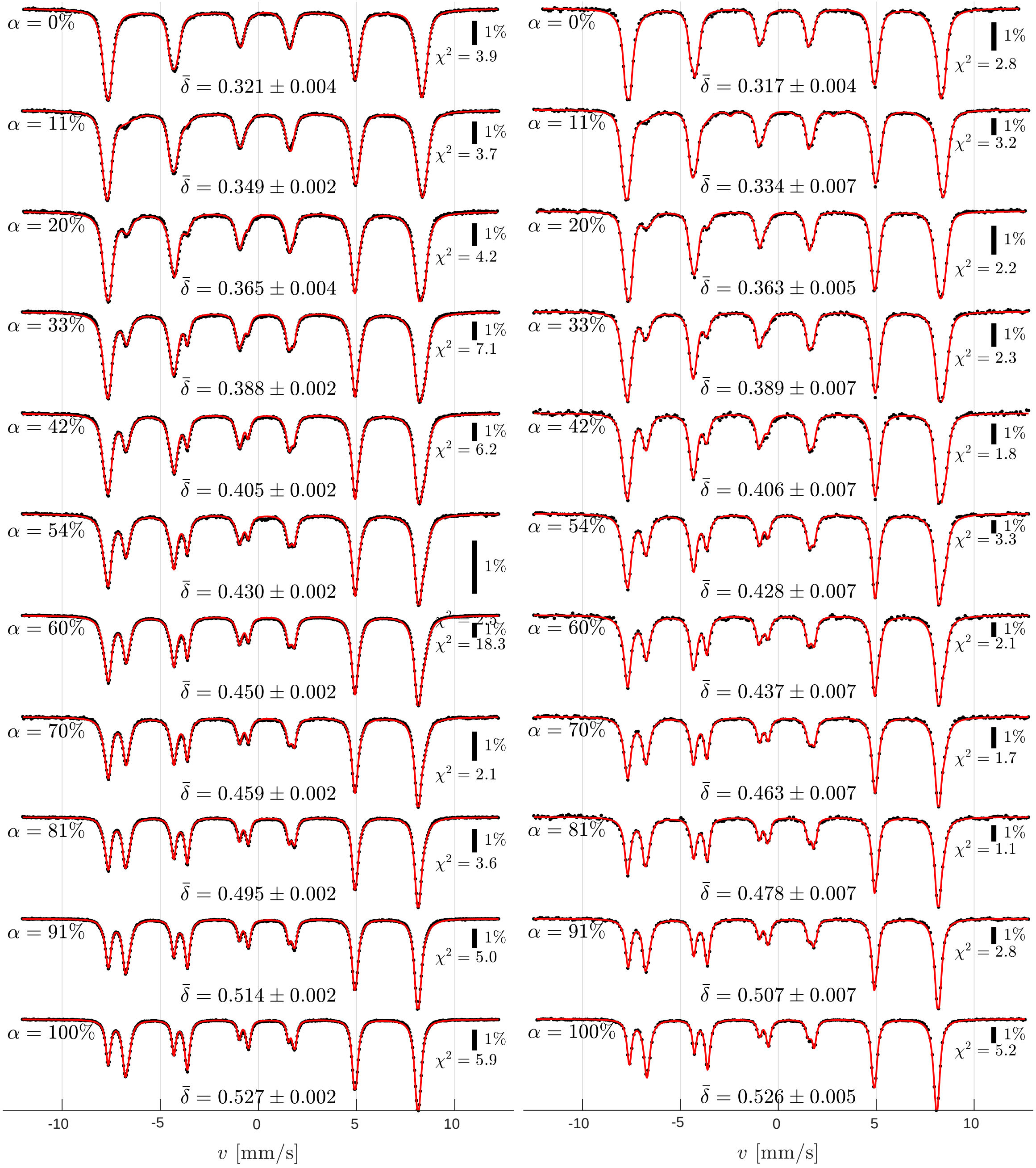

The figure above shows the full set of Mössbauer spectra of magnetite/maghemite mixtures as they were fitted at DTU. Left: UCL data fitted at DTU. Right: DTU data fitted at DTU.

The parameters obtained from fits of the Mössbauer spectra for the UCL data fitted at DTU are given below (and following the notation defined in main text and in Section S2(b)):

Voigtian line fit						
a = 0 %	**MSE = 3.9**	**$\bar{\delta}$ = 0.321 ± 0.004 mm/s**		**Lorentzian: γ = 0.174 mm/s**		
δ [mm/s]	ε [mm/s]	$\mu_0 H_{\mathrm{hf}}$ [T]	$2\sigma_{1,6}$ [mm/s]	$2\sigma_{2,5}$ [mm/s]	$2\sigma_{3,4}$ [mm/s]	Area [%]
0.271 ± 0.002	0.08 ± 0.00	50.69 ± 0.08	0.02 ± 0.13	0.01 ± 0.07	0.00 ± 0.02	13.98 ± 1.97
		49.42 ± 0.06	0.06 ± 0.04	0.03 ± 0.03	0.01 ± 0.01	18.91 ± 2.08
0.346 ± 0.001	-0.05 ± 0.00	49.36 ± 0.01	0.40 ± 0.00	0.23 ± 0.00	0.06 ± 0.00	51.83 ± 0.76
		36.46 ± 0.61	4.94 ± 0.15	2.86 ± 0.09	0.78 ± 0.02	15.28 ± 0.64

Voigtian line fit						
a = 11 %	**MSE = 3.7**	**$\bar{\delta}$ = 0.349 ± 0.002 mm/s**		**Lorentzian: γ = 0.167 mm/s**		
δ [mm/s]	ε [mm/s]	$\mu_0 H_{\mathrm{hf}}$ [T]	$2\sigma_{1,6}$ [mm/s]	$2\sigma_{2,5}$ [mm/s]	$2\sigma_{3,4}$ [mm/s]	Area [%]
0.302 ± 0.002	0.10 ± 0.00	51.01 ± 0.25	0.09 ± 0.07	0.05 ± 0.04	0.01 ± 0.01	8.38 ± 4.51
		49.78 ± 0.13	0.15 ± 0.03	0.09 ± 0.02	0.02 ± 0.00	25.10 ± 4.60
0.307 ± 0.002	-0.09 ± 0.00	49.71 ± 0.01	0.29 ± 0.01	0.17 ± 0.00	0.05 ± 0.00	40.54 ± 0.91
		35.28 ± 0.92	5.72 ± 0.20	3.31 ± 0.12	0.91 ± 0.03	12.76 ± 0.71
0.632 ± 0.008	0.06 ± 0.01	46.86 ± 0.09	0.90 ± 0.03	0.52 ± 0.02	0.14 ± 0.00	13.21 ± 0.42

Lorentzian line fit						
a = 20 %	**MSE = 4.2**	**$\bar{\delta}$ = 0.365 ± 0.004 mm/s**				
δ [mm/s]	ε [mm/s]	$\mu_0 H_{\mathrm{hf}}$ [T]	$2\gamma_{1,6}$ [mm/s]	$2\gamma_{2,5}$ [mm/s]	$2\gamma_{3,4}$ [mm/s]	Area [%]
0.309 ± 0.002	0.02 ± 0.00	50.43 ± 0.03	0.42 ± 0.01	0.50 ± 0.01	0.44 ± 0.02	34.80 ± 1.94
0.313 ± 0.001	-0.01 ± 0.00	48.94 ± 0.03	0.46 ± 0.01	0.42 ± 0.01	0.44 ± 0.02	48.61 ± 2.13
0.634 ± 0.004	0.02 ± 0.00	45.57 ± 0.03	0.58 ± 0.02	0.44 ± 0.02	0.33 ± 0.01	16.59 ± 0.43

Lorentzian line fit						
a = 33 %	**MSE = 7.1**	**$\bar{\delta}$ = 0.388 ± 0.002 mm/s**				
δ [mm/s]	ε [mm/s]	$\mu_0 H_{\mathrm{hf}}$ [T]	$2\gamma_{1,6}$ [mm/s]	$2\gamma_{2,5}$ [mm/s]	$2\gamma_{3,4}$ [mm/s]	Area [%]
0.248 ± 0.002	-0.01 ± 0.00	49.58 ± 0.01	0.50 ± 0.00	0.43 ± 0.00	0.36 ± 0.00	55.32 ± 0.96
0.460 ± 0.003	-0.00 ± 0.00	49.91 ± 0.01	0.38 ± 0.01	0.39 ± 0.01	0.35 ± 0.01	22.40 ± 0.90
0.664 ± 0.001	0.02 ± 0.00	45.86 ± 0.01	0.46 ± 0.01	0.31 ± 0.00	0.29 ± 0.01	22.28 ± 0.19

Lorentzian line fit						
a = 42 %	**MSE = 6.2**	**$\bar{\delta}$ = 0.405 ± 0.002 mm/s**				
δ [mm/s]	ε [mm/s]	$\mu_0 H_{\mathrm{hf}}$ [T]	$2\gamma_{1,6}$ [mm/s]	$2\gamma_{2,5}$ [mm/s]	$2\gamma_{3,4}$ [mm/s]	Area [%]
0.285 ± 0.003	0.03 ± 0.00	50.58 ± 0.03	0.40 ± 0.01	0.44 ± 0.01	0.40 ± 0.01	24.28 ± 1.34
0.299 ± 0.001	-0.02 ± 0.00	49.14 ± 0.01	0.42 ± 0.01	0.38 ± 0.00	0.37 ± 0.01	48.04 ± 1.40
0.638 ± 0.002	0.00 ± 0.00	45.98 ± 0.01	0.42 ± 0.01	0.38 ± 0.01	0.23 ± 0.01	21.66 ± 0.61
0.901 ± 0.005	0.11 ± 0.00	47.19 ± 0.03	0.38 ± 0.02	0.22 ± 0.01	0.25 ± 0.02	6.02 ± 0.52

Lorentzian line fit						
a = 54 %	**MSE = 2.5**	**$\bar{\delta}$ = 0.430 ± 0.002 mm/s**				
δ [mm/s]	ε [mm/s]	$\mu_0 H_{hf}$ [T]	$2\gamma_{1,6}$ [mm/s]	$2\gamma_{2,5}$ [mm/s]	$2\gamma_{3,4}$ [mm/s]	Area [%]
0.281 ± 0.002	-0.00 ± 0.00	49.11 ± 0.02	0.38 ± 0.01	0.34 ± 0.01	0.34 ± 0.01	37.09 ± 1.28
0.337 ± 0.003	0.00 ± 0.00	50.54 ± 0.04	0.47 ± 0.01	0.53 ± 0.01	0.48 ± 0.03	28.37 ± 1.36
0.667 ± 0.002	0.01 ± 0.00	46.04 ± 0.01	0.44 ± 0.01	0.33 ± 0.00	0.28 ± 0.01	34.54 ± 0.31

Lorentzian line fit						
a = 60 %	**MSE = 18.3**	**$\bar{\delta}$ = 0.450 ± 0.002 mm/s**				
δ [mm/s]	ε [mm/s]	$\mu_0 H_{hf}$ [T]	$2\gamma_{1,6}$ [mm/s]	$2\gamma_{2,5}$ [mm/s]	$2\gamma_{3,4}$ [mm/s]	Area [%]
0.275 ± 0.001	0.00 ± 0.00	49.07 ± 0.00	0.38 ± 0.00	0.34 ± 0.00	0.31 ± 0.00	36.86 ± 0.39
0.356 ± 0.001	-0.01 ± 0.00	50.47 ± 0.01	0.48 ± 0.00	0.54 ± 0.01	0.44 ± 0.01	23.56 ± 0.42
0.668 ± 0.000	0.01 ± 0.00	45.95 ± 0.00	0.43 ± 0.00	0.32 ± 0.00	0.28 ± 0.00	39.58 ± 0.10

Lorentzian line fit						
a = 70 %	**MSE = 2.1**	**$\bar{\delta}$ = 0.459 ± 0.002 mm/s**				
δ [mm/s]	ε [mm/s]	$\mu_0 H_{hf}$ [T]	$2\gamma_{1,6}$ [mm/s]	$2\gamma_{2,5}$ [mm/s]	$2\gamma_{3,4}$ [mm/s]	Area [%]
0.273 ± 0.001	-0.00 ± 0.00	49.05 ± 0.01	0.35 ± 0.01	0.31 ± 0.01	0.31 ± 0.01	37.06 ± 1.13
0.351 ± 0.005	-0.02 ± 0.00	50.43 ± 0.05	0.45 ± 0.02	0.49 ± 0.02	0.36 ± 0.02	19.76 ± 1.23
0.668 ± 0.001	0.01 ± 0.00	45.97 ± 0.01	0.41 ± 0.00	0.31 ± 0.00	0.27 ± 0.00	43.17 ± 0.31

Voigtian line fit						
a = 81 %	**MSE = 3.6**	**$\bar{\delta}$ = 0.495 ± 0.002 mm/s**		**Lorentzian: γ = 0.120 mm/s**		
δ [mm/s]	ε [mm/s]	$\mu_0 H_{hf}$ [T]	$2\sigma_{1,6}$ [mm/s]	$2\sigma_{2,5}$ [mm/s]	$2\sigma_{3,4}$ [mm/s]	Area [%]
0.284 ± 0.001	-0.00 ± 0.00	49.18 ± 0.02	0.13 ± 0.01	0.07 ± 0.01	0.02 ± 0.00	32.74 ± 3.48
		50.45 ± 0.31	0.26 ± 0.05	0.15 ± 0.03	0.04 ± 0.01	11.47 ± 3.50
0.654 ± 0.001	0.04 ± 0.00	47.33 ± 0.08	0.99 ± 0.02	0.57 ± 0.01	0.16 ± 0.00	15.14 ± 0.46
		45.44 ± 0.04	0.14 ± 0.01	0.08 ± 0.01	0.02 ± 0.00	16.94 ± 1.10
0.671 ± 0.001	-0.02 ± 0.00	46.27 ± 0.01	0.10 ± 0.01	0.06 ± 0.00	0.02 ± 0.00	23.71 ± 1.02

Voigtian line fit						
a = 91 %	**MSE = 5.0**	**$\bar{\delta}$ = 0.514 ± 0.002 mm/s**		**Lorentzian: γ = 0.118 mm/s**		
δ [mm/s]	ε [mm/s]	$\mu_0 H_{hf}$ [T]	$2\sigma_{1,6}$ [mm/s]	$2\sigma_{2,5}$ [mm/s]	$2\sigma_{3,4}$ [mm/s]	Area [%]
0.282 ± 0.001	-0.00 ± 0.00	49.19 ± 0.02	0.13 ± 0.01	0.08 ± 0.00	0.02 ± 0.00	33.36 ± 1.65
		50.64 ± 0.31	0.26 ± 0.06	0.15 ± 0.03	0.04 ± 0.01	5.76 ± 1.66
0.658 ± 0.001	0.04 ± 0.00	47.07 ± 0.06	1.03 ± 0.02	0.60 ± 0.01	0.16 ± 0.00	15.44 ± 0.36
		45.50 ± 0.03	0.18 ± 0.01	0.10 ± 0.00	0.03 ± 0.00	19.57 ± 0.98
0.672 ± 0.001	-0.03 ± 0.00	46.20 ± 0.01	0.11 ± 0.01	0.07 ± 0.00	0.02 ± 0.00	25.86 ± 0.93

Voigtian line fit						
a = 100 %	**MSE = 5.9**	**$\bar{\delta}$ = 0.527 ± 0.002 mm/s**				
δ [mm/s]	ε [mm/s]	$\mu_0 H_{\mathrm{hf}}$ [T]	$2\gamma_{1,6}$ [mm/s]	$2\gamma_{2,5}$ [mm/s]	$2\gamma_{3,4}$ [mm/s]	Area [%]
0.265 ± 0.000	-0.01 ± 0.00	49.11 ± 0.00	0.29 ± 0.00	0.25 ± 0.00	0.23 ± 0.00	36.17 ± 0.13
0.665 ± 0.001	-0.03 ± 0.00	46.10 ± 0.00	0.34 ± 0.00	0.27 ± 0.00	0.24 ± 0.00	46.18 ± 0.96
0.702 ± 0.001	0.12 ± 0.00	46.09 ± 0.01	0.34 ± 0.01	0.31 ± 0.01	0.20 ± 0.01	17.65 ± 0.95

S8. Linear regression calculation

The linear regression for the relation between δ_{RT} and α/α_2 (where α_2 is the α value of the DTU100 magnetite sample) for the mixtures of

$$\delta_{RT}(\alpha) = m' \frac{\alpha}{\alpha_2} + \delta_0 \tag{S8.1}$$

was obtained by calculating the weighted mean of $\bar{\delta}_{RT}(\alpha)$ for the four mean isomer shifts obtained from the fits obtained at UCL and DTU from the two independent measurements at UCL and DTU as,

$$\bar{\delta}_{RT} = \frac{\sum_n \delta_n \ \mathrm{d}\delta_n^{-2}}{\sum_n \mathrm{d}\delta_n^{-2}} \quad , \tag{S8.2}$$

and the variance

$$\mathrm{d}\delta_{RT}^2 = \frac{2}{\sum \ \mathrm{d}\delta_n^{-2}} \quad , \tag{S8.3}$$

where the factor of 2 arises from the fact that the data points are correlated because the same dataset is fitted twice.

The slope and intercept m and δ_0 were determined from linear regression of the data points (α_i, δ_i) with uncertainty $\mathrm{d}\delta_i$ by minimising the sum of square of residuals, ϵ:

$$\mathbf{A} \begin{vmatrix} m' \\ \delta_0 \end{vmatrix} = \mathbf{W} \begin{vmatrix} \delta_1 \\ \vdots \\ \delta_N \end{vmatrix} + \epsilon, \tag{S8.4}$$

where

$$\begin{vmatrix} m' \\ \delta_0 \end{vmatrix} = \left(\mathbf{A}^{\mathrm{T}}\mathbf{A}\right)^{-1} \mathbf{A}^{\mathrm{T}}\mathbf{W} \begin{vmatrix} \delta_1 \\ \vdots \\ \delta_N \end{vmatrix} \tag{S8.5}$$

and

$$\mathbf{A} = \mathbf{W} \begin{vmatrix} \alpha_1 & 1 \\ \vdots & \\ \alpha_N & 1 \end{vmatrix}. \tag{S8.6}$$

The weighting matrix is

$$\mathbf{W} = \begin{vmatrix} w_{11} & 0 & 0 \\ 0 & \ddots & 0 \\ 0 & 0 & w_{NN} \end{vmatrix} \tag{S8.7}$$

with $w_{ii} = \mathrm{d}\delta_{RT}^{-2}(\alpha_i)$.

The covariance matrix is

$$\Sigma = \left(\mathbf{A}^{\mathrm{T}}\mathbf{A}\right)^{-1}. \tag{S8.8}$$

Finally, the confidence intervals on m and δ_0 are

$$t_{p/2}\sqrt{[\alpha\ 1]\boldsymbol{\Sigma}\,[\alpha\ 1]^{\mathrm{T}}}\,, \tag{S8.9}$$

where $t_{p/2}$ is the $100(1\ -\ p/2)$th percentile of Student's t-distribution.

From Eq. (S8.1) it follows that $m = m'/\alpha_2$ is the slope of δ_{RT} versus α.

S9. Temperature dependence analysis

First, we define the reduced temperature

$$t = \frac{T}{T_0}. \tag{S9.1}$$

S9(a). Magnetite

The temperature dependence of the 97% pure magnetite ($\alpha_2 = 0.97$) was measured and could phenomenologically be described by a simple parabolic model

$$\bar{\delta}_2(t) = a_2(1 - t^2) + (m' + \delta_o)\, t^2 \tag{S9.2}$$

where $a_2 = 0.641 \pm 0.002$ mm/s. The temperature dependence of the 100% pure magnetite can then be deduced by assuming linear dependence between α and $\bar{\delta}$ as

$$\bar{\delta}_{\mathrm{Fe_3O_4}}(t) = \frac{\bar{\delta}_2(t) - \bar{\delta}_{\gamma\text{-}\mathrm{Fe_2O_3}}(t)}{\alpha_2} + \bar{\delta}_{\gamma\text{-}\mathrm{Fe_2O_3}}(t) \tag{S9.3}$$

$$\bar{\delta}_\alpha(t) = \frac{a_2(1 - t^2) + m'\, t^2 - a_{\gamma\text{-}\mathrm{Fe_2O_3}}(1 - t^2)}{\alpha_2} + a_{\gamma\text{-}\mathrm{Fe_2O_3}}(1 - t^2) + \delta_o\, t^2 \tag{S9.4}$$

$$\bar{\delta}_{\mathrm{Fe_3O_4}}(t) = a_{\mathrm{Fe_3O_4}}(1 - t^2) + (m + \delta_o)\, t^2 \tag{S9.5}$$

where

$$a_{\mathrm{Fe_3O_4}} = \frac{a_2 + (\alpha_2 - 1)a_{\gamma\text{-}\mathrm{Fe_2O_3}}}{\alpha_2} = 0.647 \pm 0.002 \text{ mm/s} \tag{S9.6}$$

Eq. (S9.5) corresponds to Eq. (16a) in the text.

S9(b). Uncertainty calculation of determination of *α*(*T*)

The atomic Fe content in magnetite can be expressed as

$$\alpha = \frac{\bar{\delta}(T) - \delta_0(t)}{m(t)} \pm \mathrm{d}\alpha\,, \tag{S9.7}$$

with

$$m(t) = \frac{\left(a_{\alpha_2} - a_{\alpha_1}\right)(1 - t^2) + m' t^2}{\Delta\alpha} \tag{S9.8}$$

and

$$m' = \delta_{0\alpha_2} - \delta_{0\alpha_1} \tag{S9.9}$$

and

$$\delta_0(t) = \frac{\alpha_2\left(a_{\alpha_1}(1 - t^2) + \delta_{0\alpha_1} t^2\right) - \alpha_1\left(a_{\alpha_2}(1 - t^2) + (\delta_{0\alpha_1} + m')t^2\right)}{\Delta\alpha} \tag{S9.10}$$

where $\alpha_1 = 0.00 \pm 0.01$ and $\alpha_2 = 0.97 \pm 0.02$ are the α values of DTU0 and DTU100 respectively and $\Delta\alpha = \alpha_2 - \alpha_1$. $\delta_{0\alpha_2}$and $\delta_{0\alpha_1}$ are the mean isomer shifts at $t = 1$ whereas a_{α_1} and a_{α_2} are the mean isomer shifts for $t = 0$ for DTU0 and DTU100 respectively.

Thus

$$\alpha = \frac{\bar{\delta}(T) - \frac{\alpha_2}{\Delta\alpha}\left(a_{\alpha_1}(1-t^2) + \delta_{0\alpha_1}t^2\right) + \frac{\alpha_1}{\Delta\alpha}\left(a_{\alpha_2}(1-t^2) + \left(\delta_{0\alpha_1} + m'\right) t^2\right)}{\left(a_{\alpha_2} - a_{\alpha_1}\right)(1-t^2)/\Delta\alpha + m'/\Delta\alpha\, t^2} \pm \mathrm{d}\alpha \tag{S9.11}$$

The uncertainty on α is given by

$$(\mathrm{d}\alpha)^2 = J\,\mathbf{\Sigma}\,J^{\mathrm{T}}, \tag{S9.12}$$

where $\mathbf{\Sigma}$ is the covariance matrix

$$\mathbf{\Sigma} = \begin{vmatrix} \sigma_{\bar{\delta}\bar{\delta}} & 0 & 0 & 0 & 0 & 0 & 0 & 0 \\ 0 & \mathrm{d}a_{\alpha_1}^2 & 0 & 0 & 0 & 0 & 0 & 0 \\ 0 & 0 & \mathrm{d}a_{\alpha_2}^2 & 0 & 0 & 0 & 0 & 0 \\ 0 & 0 & 0 & \mathrm{d}t^2 & 0 & 0 & 0 & 0 \\ 0 & 0 & 0 & 0 & \sigma_{m'm'} & \sigma_{m'\delta_{0\alpha_1}} & 0 & 0 \\ 0 & 0 & 0 & 0 & \sigma_{m'\delta_{0\alpha_1}} & \sigma_{\delta_0\delta_{0\alpha_1}} & 0 & 0 \\ 0 & 0 & 0 & 0 & 0 & 0 & \sigma_{\alpha_1\alpha_1} & 0 \\ 0 & 0 & 0 & 0 & 0 & 0 & 0 & \sigma_{\alpha_2\alpha_2} \end{vmatrix}, \tag{S9.13}$$

and the Jacobian is

$$J = \left[\frac{\mathrm{d}\alpha}{\mathrm{d}\bar{\delta}(T)}\,, \frac{\mathrm{d}\alpha}{\mathrm{d}a_{\alpha_1}}\,, \frac{\mathrm{d}\alpha}{\mathrm{d}a_{\alpha_2}}, \frac{\mathrm{d}\alpha}{\mathrm{d}t}, \frac{\mathrm{d}\alpha}{\mathrm{d}m'}, \frac{\mathrm{d}\alpha}{\delta_{0\alpha_1}}, \frac{\mathrm{d}\alpha}{\alpha_1}\ \frac{\mathrm{d}\alpha}{\alpha_2}\right]. \tag{S9.14}$$

The terms in the Jacobian are

$$\frac{\mathrm{d}\alpha}{\mathrm{d}\bar{\delta}(T)} = \frac{\Delta\alpha}{\left(a_{\alpha_2} - a_{\alpha_1}\right)(1-t^2) + m'\,t^2} \tag{S9.15}$$

$$\frac{\mathrm{d}\alpha}{\mathrm{d}a_{\alpha_1}} = \frac{-(1-t^2)(\alpha_2 - \alpha)}{\left(a_{\alpha_2} - a_{\alpha_1}\right)(1-t^2) + m'\,t^2} \tag{S9.16}$$

$$\frac{\mathrm{d}\alpha}{\mathrm{d}a_{\alpha_2}} = \frac{-(1-t^2)(\alpha_1 + \alpha)}{\left(a_{\alpha_2} - a_{\alpha_1}\right)(1-t^2) + m'\,t^2} \tag{S9.17}$$

$$\frac{\mathrm{d}\alpha}{\mathrm{d}t} = 2t\,\frac{\alpha_2\left(a_{\alpha_1} - \delta_{0\alpha_1}\right) - \alpha_1\left(a_{\alpha_2} - \left(\delta_{0\alpha_1} + m'\right)\right) - \left(m - \left(a_{\alpha_2} - a_{\alpha_1}\right)\right)\alpha}{\left(a_{\alpha_2} - a_{\alpha_1}\right)(1-t^2) + m'\,t^2} \tag{S9.18}$$

$$\frac{\mathrm{d}\alpha}{\mathrm{d}m'} = t^2\,\frac{\alpha}{\left(a_{\alpha_2} - a_{\alpha_1}\right)(1-t^2) + m'\,t^2} \tag{S9.19}$$

$$\frac{d\alpha}{\mathrm{d}\delta_{\mathrm{o}}} = \frac{-\Delta p\,t^2}{\left(a_{\alpha_2} - a_{\alpha_1}\right)(1-t^2) + m'\,t^2} \tag{S9.20}$$

$$\frac{d\alpha}{d\alpha_1} = \frac{-\bar{\delta}(T) + a_{\alpha_2}(1-t^2) + \left(\delta_{0\alpha_1} \ \ + m'\ \right)t^2}{\left(a_{\alpha_2} - a_{\alpha_1}\right)(1-t^2) + m'\, t^2} \tag{S9.21}$$

$$\frac{d\alpha}{d\alpha_2} = \frac{\bar{\delta}(T) - \left(a_{\alpha_1}(1-t^2) + \delta_{0\alpha_1}t^2\right)}{\left(a_{\alpha_2} - a_{\alpha_1}\right)(1-t^2) + m'\, t^2} \tag{S9.22}$$

Inserting the numerical values, we can estimate an upper limit of the uncertainty as

$$\begin{gathered} \mathrm{d}\alpha < \sqrt{22\,(\mathrm{d}\delta)^2 + \ 0.018\left|\delta - a_{\alpha_1}(1-t^2) - \delta_o\, t^2 - 0.035 + i\,0.13\right|^2}\ , \\ \mathrm{d}\alpha < \ \sqrt{22\,(\mathrm{d}\delta)^2 + \ 0.030^2} \quad \text{for} \quad \mathrm{d}T < 3\ \mathrm{K}. \end{gathered} \tag{S9.23}$$

When $T = T_0$ and $\mathrm{d}T = 0$, the expression reduces to

$$\begin{gathered} \mathrm{d}\alpha < \sqrt{22\,(\mathrm{d}\delta)^2 + \ 0.018\,|\delta - \delta_o \ - 0.028 + i\,0.08|^2} \\ \mathrm{d}\alpha < \sqrt{22\,(\mathrm{d}\delta)^2 + \ 0.027^2}\ . \end{gathered} \tag{S9.24}$$

S10. Variable temperature Mössbauer data for commercial sample MM03

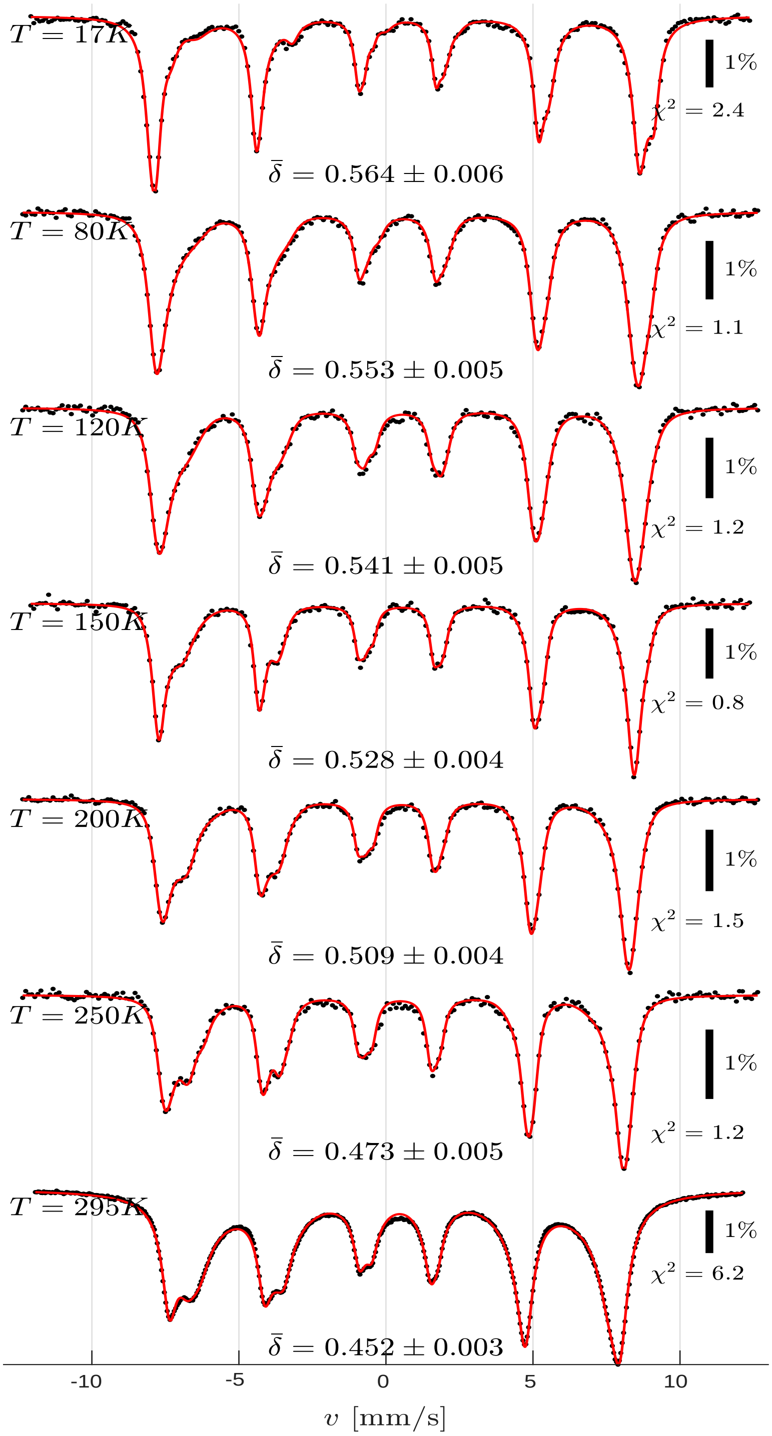

The parameters obtained from fits of the Mössbauer spectra are given below (and following the notation defined in main text and in Section S4):

Lorentzian line fit						
T = 17 K	**MSE = 2.4**	**$\bar{\delta}$ = 0.564 ± 0.006 mm/s**				
δ [mm/s]	ε [mm/s]	$\mu_0 H_{hf}$ [T]	$2\gamma_{1,6}$ [mm/s]	$2\gamma_{2,5}$ [mm/s]	$2\gamma_{3,4}$ [mm/s]	Area [%]
0.354 ± 0.004	-0.03 ± 0.00	51.45 ± 0.02	0.54 ± 0.01	0.44 ± 0.01	0.37 ± 0.01	53.68 ± 2.34
0.628 ± 0.006	0.03 ± 0.00	52.51 ± 0.03	0.41 ± 0.02	0.53 ± 0.03	0.32 ± 0.03	24.01 ± 2.87
0.807 ± 0.021	-0.03 ± 0.02	50.16 ± 0.27	0.57 ± 0.08	0.91 ± 0.11	0.29 ± 0.04	10.59 ± 1.69
1.176 ± 0.028	-0.03 ± 0.02	47.03 ± 0.18	1.02 ± 0.10	0.52 ± 0.06	0.54 ± 0.08	11.71 ± 1.11

Voigtian line fit						
T = 80 K	**MSE = 1.1**	**$\bar{\delta}$ = 0.553 ± 0.005 mm/s**		**Lorentzian: γ = 0.220 mm/s**		
δ [mm/s]	ε [mm/s]	$\mu_0 H_{hf}$ [T]	$2\sigma_{1,6}$ [mm/s]	$2\sigma_{2,5}$ [mm/s]	$2\sigma_{3,4}$ [mm/s]	Area [%]
0.386 ± 0.009	0.01 ± 0.01	50.78 ± 0.05	0.37 ± 0.02	0.22 ± 0.01	0.06 ± 0.00	54.13 ± 2.76
0.603 ± 0.016	-0.02 ± 0.01	52.29 ± 0.12	0.09 ± 0.12	0.05 ± 0.07	0.01 ± 0.02	11.51 ± 3.37
0.639 ± 0.036	-0.03 ± 0.02	49.32 ± 0.52	0.51 ± 0.14	0.29 ± 0.08	0.08 ± 0.02	16.62 ± 4.46
0.951 ± 0.033	-0.00 ± 0.02	47.25 ± 0.29	0.83 ± 0.08	0.48 ± 0.04	0.13 ± 0.01	17.73 ± 2.48

Voigtian line fit						
T = 120 K	**MSE = 1.2**	**$\bar{\delta}$ = 0.541 ± 0.005 mm/s**		**Lorentzian: γ = 0.212 mm/s**		
δ [mm/s]	ε [mm/s]	$\mu_0 H_{hf}$ [T]	$2\sigma_{1,6}$ [mm/s]	$2\sigma_{2,5}$ [mm/s]	$2\sigma_{3,4}$ [mm/s]	Area [%]
0.314 ± 0.015	0.02 ± 0.01	50.27 ± 0.05	0.30 ± 0.03	0.17 ± 0.02	0.05 ± 0.00	32.87 ± 4.38
0.529 ± 0.028	-0.01 ± 0.01	50.38 ± 0.08	0.51 ± 0.05	0.30 ± 0.03	0.08 ± 0.01	36.17 ± 3.98
0.796 ± 0.014	-0.01 ± 0.01	47.35 ± 0.25	0.82 ± 0.06	0.48 ± 0.03	0.13 ± 0.01	30.96 ± 2.64

Voigtian line fit						
T = 150 K	**MSE = 0.8**	**$\bar{\delta}$ = 0.528 ± 0.004 mm/s**		**Lorentzian: γ = 0.167 mm/s**		
δ [mm/s]	ε [mm/s]	$\mu_0 H_{hf}$ [T]	$2\sigma_{1,6}$ [mm/s]	$2\sigma_{2,5}$ [mm/s]	$2\sigma_{3,4}$ [mm/s]	Area [%]
0.348 ± 0.006	0.01 ± 0.01	50.15 ± 0.05	0.19 ± 0.02	0.11 ± 0.01	0.03 ± 0.00	37.36 ± 3.15
0.473 ± 0.025	-0.07 ± 0.02	50.88 ± 0.17	0.38 ± 0.06	0.22 ± 0.04	0.06 ± 0.01	17.69 ± 4.13
0.661 ± 0.026	0.11 ± 0.03	46.23 ± 0.84	0.97 ± 0.19	0.56 ± 0.11	0.15 ± 0.03	14.96 ± 4.33
		50.60 ± 0.19	0.15 ± 0.17	0.09 ± 0.10	0.02 ± 0.03	5.38 ± 3.42
0.729 ± 0.013	-0.05 ± 0.02	47.56 ± 0.15	0.54 ± 0.07	0.31 ± 0.04	0.09 ± 0.01	24.61 ± 3.51

Voigtian line fit						
T = 200 K	**MSE = 1.5**	**$\bar{\delta}$ = 0.509 ± 0.004 mm/s**		**Lorentzian: γ = 0.184 mm/s**		
δ [mm/s]	ε [mm/s]	$\mu_0 H_{hf}$ [T]	$2\sigma_{1,6}$ [mm/s]	$2\sigma_{2,5}$ [mm/s]	$2\sigma_{3,4}$ [mm/s]	Area [%]
0.306 ± 0.006	-0.00 ± 0.00	49.27 ± 0.03	0.29 ± 0.02	0.17 ± 0.01	0.05 ± 0.00	36.68 ± 2.74
0.492 ± 0.028	-0.03 ± 0.01	48.16 ± 0.24	0.63 ± 0.06	0.37 ± 0.03	0.10 ± 0.01	30.52 ± 4.02
0.662 ± 0.021	0.02 ± 0.02	43.26 ± 1.51	0.95 ± 0.24	0.55 ± 0.14	0.15 ± 0.04	12.95 ± 6.05
0.812 ± 0.016	0.02 ± 0.01	47.13 ± 0.14	0.40 ± 0.04	0.23 ± 0.02	0.06 ± 0.01	19.85 ± 2.91

Voigtian line fit						
T = 250 K	**MSE = 1.2**	**$\bar{\delta}$ = 0.473 ± 0.005 mm/s**		**Lorentzian: γ = 0.179 mm/s**		
δ [mm/s]	ε [mm/s]	$\mu_0 H_{hf}$ [T]	$2\sigma_{1,6}$ [mm/s]	$2\sigma_{2,5}$ [mm/s]	$2\sigma_{3,4}$ [mm/s]	Area [%]
0.258 ± 0.016	-0.02 ± 0.01	48.36 ± 0.05	0.27 ± 0.04	0.16 ± 0.02	0.04 ± 0.01	31.91 ± 4.30
0.474 ± 0.031	0.02 ± 0.01	43.32 ± 1.20	1.10 ± 0.23	0.64 ± 0.13	0.18 ± 0.04	19.37 ± 6.07
		48.22 ± 0.13	0.36 ± 0.11	0.21 ± 0.06	0.06 ± 0.02	18.55 ± 5.93
0.698 ± 0.012	0.00 ± 0.01	46.19 ± 0.13	0.34 ± 0.06	0.20 ± 0.03	0.05 ± 0.01	23.89 ± 2.83
		42.86 ± 0.30	0.21 ± 0.13	0.12 ± 0.07	0.03 ± 0.02	6.28 ± 2.01

Lorentzian line fit						
T = 295 K	**MSE = 6.2**	**$\bar{\delta}$ = 0.452 ± 0.003 mm/s**				
δ [mm/s]	ε [mm/s]	$\mu_0 H_{hf}$ [T]	$2\gamma_{1,6}$ [mm/s]	$2\gamma_{2,5}$ [mm/s]	$2\gamma_{3,4}$ [mm/s]	Area [%]
0.306 ± 0.001	-0.01 ± 0.00	47.60 ± 0.01	0.59 ± 0.01	0.54 ± 0.01	0.46 ± 0.01	27.33 ± 0.51
0.431 ± 0.008	-0.01 ± 0.00	44.47 ± 0.03	1.00 ± 0.04	0.97 ± 0.02	1.05 ± 0.05	32.09 ± 2.42
0.503 ± 0.008	0.01 ± 0.01	39.99 ± 0.39	2.67 ± 0.03	1.97 ± 0.03	1.03 ± 0.03	27.21 ± 2.08
0.701 ± 0.007	0.06 ± 0.01	43.88 ± 0.05	0.85 ± 0.03	0.59 ± 0.02	0.41 ± 0.02	13.36 ± 1.21

S11. Model-independent fitting of da Costa and Gorski Mössbauer data.

We are very grateful to Geraldo da Costa (Federal University of Ouro Preto, Brazil) and to Christopher Gorski and Michelle Scherer (University of Iowa, USA) for providing their raw Mössbauer data for analysis using our model-independent protocol.

S11(a). Model-independent fitting of da Costa *et al.* Mössbauer data.

Data used were the same as that in the publication:

da Costa G M, Blanco-Andujar C, De Grave E and Pankhurst Q A 2014 Magnetic nanoparticles for in vivo use: a critical assessment of their composition *Journal of Physical Chemistry B* **118** 11738-46.

Model-independent fits were performed on the spectra, as below:

Sample	**% magnetite (Fe, chemical determination)**	**Fe^{2+}**	**Fe^{3+}**	x	α	$\bar{\delta}_{RT}$ **(mm/s) (*da Costa*)**	**Uncertainty (mm/s)**	$\bar{\delta}_{RT}$ **(mm/s) (*Model independent analysis*)**	**Uncertainty (mm/s)**
Ca7	39.10	8.60	56.00	0.15	0.40	0.4019	0.01	0.4141	0.01
Ca7-100	25.30	5.60	59.00	0.09	0.26	0.3690	0.01	0.3941	0.01
Ca7-150	1.50	0.34	64.30	0.01	0.02	0.3454	0.01	0.3266	0.01
Ca7-200	1.70	0.39	64.20	0.01	0.02	0.3530	0.01	0.3209	0.01
Ca7-250	0.30	0.08	64.60	0.00	0.00	0.3400	0.01	0.3187	0.01
Ca8	81.10	19.40	51.90	0.37	0.82	0.5170	0.01	0.5008	0.01
Ca8-100	77.70	18.60	52.70	0.35	0.78	0.5118	0.01	0.4819	0.01
Ca8-150	32.50	7.90	63.40	0.12	0.33	0.4010	0.01	0.3726	0.01
Ca8-200	30.00	7.30	64.00	0.11	0.31	0.4040	0.01	0.3878	0.01
Ca8-250	2.00	0.47	70.80	0.01	0.02	0.3398	0.01	0.3192	0.01
Ca10	77.10	18.30	52.40	0.35	0.78	0.5131	0.01	0.4953	0.01
Ca10-100	69.70	16.60	54.10	0.31	0.70	0.5020	0.01	0.4796	0.01
Ca10-150	29.70	6.50	64.20	0.10	0.28	0.3867	0.01	0.3753	0.01
Ca10-200	10.30	2.50	68.20	0.04	0.11	0.3694	0.01	0.3488	0.01
Ca10-250	0.20	0.04	70.70	0.00	0.00	0.3396	0.01	0.3268	0.01

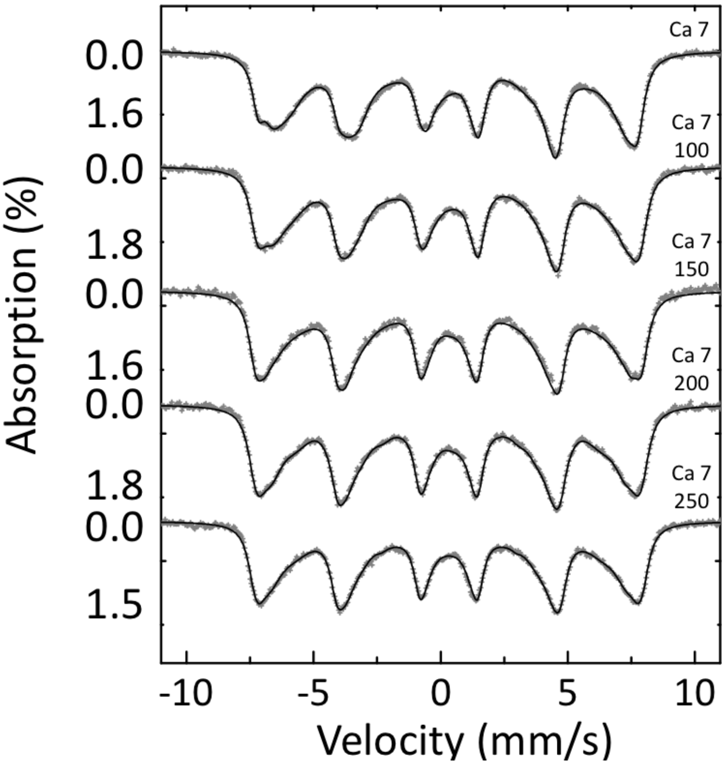
Ca 7
Ca 7 100
Ca 7 150
Ca 7 200
Ca 7 250
0.0
1.6
0.0
1.8
0.0
1.6
0.0
1.8
0.0
1.5
Absorption (%)
-10
-5
0
5
10
Velocity (mm/s)

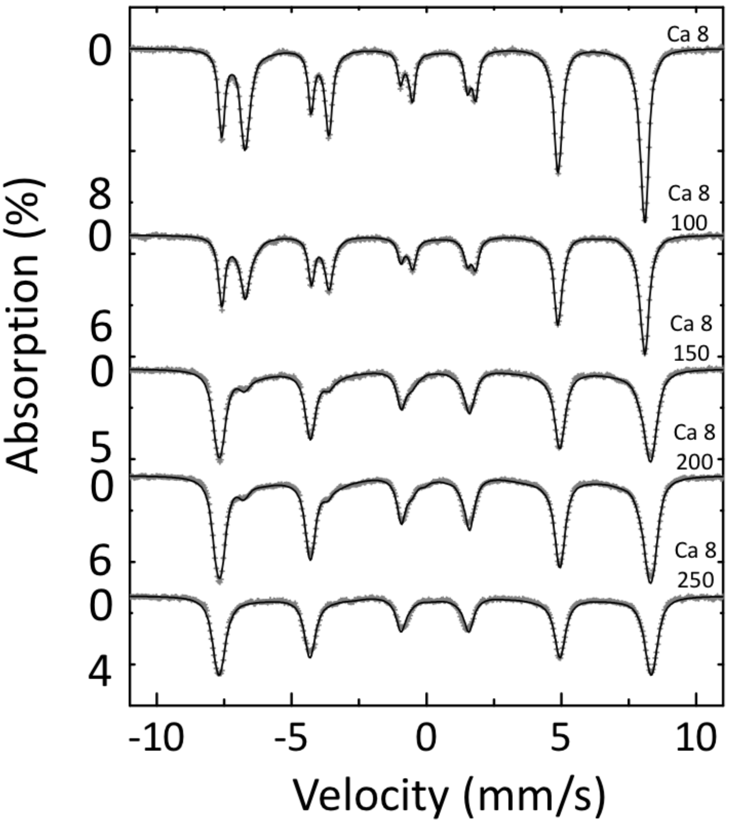
Ca 8
Ca 8 100
Ca 8 150
Ca 8 200
Ca 8 250
0
8
0
6
0
5
0
6
0
4
Absorption (%)
-10
-5
0
5
10
Velocity (mm/s)

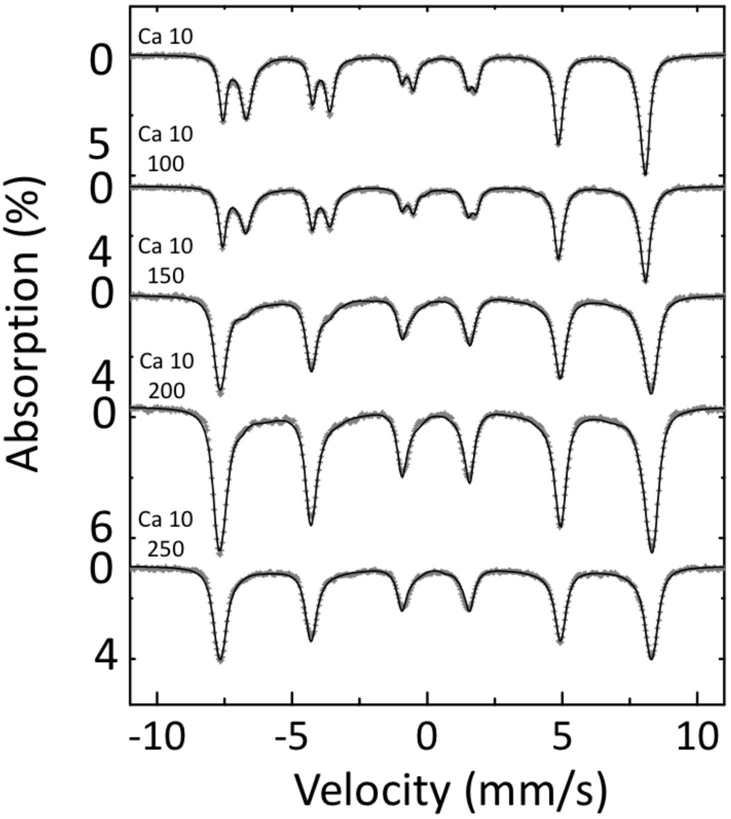

S11(b). Model-independent fitting of Gorski & Scherer Mössbauer data.

Data used were the same as that in the publication:

Gorski C A and Scherer M M 2010 Determination of nanoparticulate magnetite stoichiometry by Mossbauer spectroscopy, acidic dissolution, and powder X-ray diffraction: A critical review *American Mineralogist* **95** 1017-26.

Model-independent fits were performed on the spectra, as below:

Sample	x_D	α	$\bar{\delta}_{140K}$ **(mm/s) (*Gorski)***	$\bar{\delta}_{140K}$ **(mm/s) (*Model independent analysis*)**	**Uncertainty (mm/s)**
x 0	0	0	0.42	0.422	0.005
x 017	0.16	0.41	0.50	0.482	0.025
x 022	0.25	0.60	0.52	0.518	0.025
x 028	0.26	0.62	0.53	0.539	0.020
x 036	0.36	0.79	0.58	0.561	0.025
x 042	0.42	0.89	0.57	0.570	0.015
x 049	0.49	0.99	0.60	0.587	0.020
x 050	0.5	1	0.60	0.590	0.015

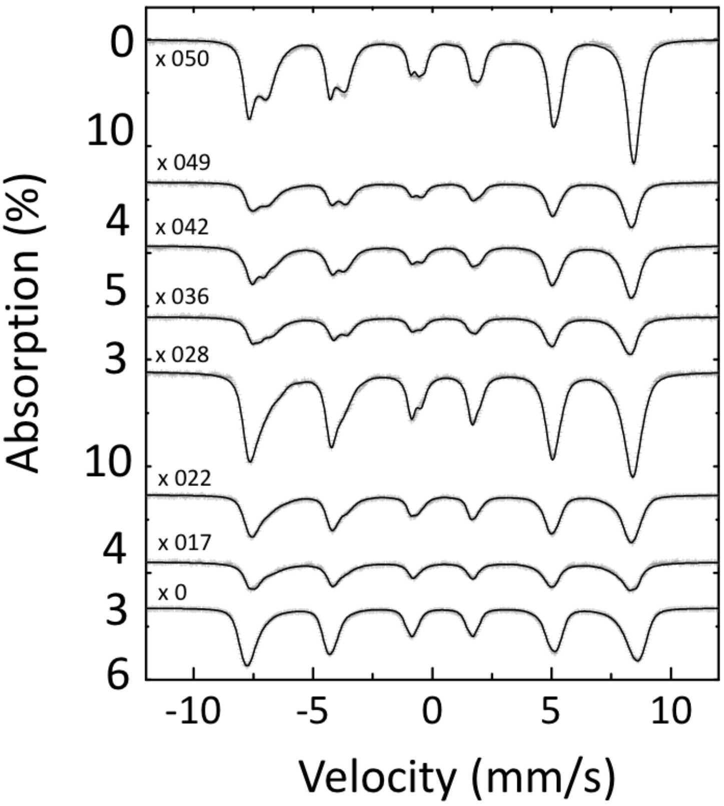
Absorption (%)
0
x 050
10
x 049
4
x 042
5
x 036
3
x 028
10
x 022
4
x 017
3
x 0
6
-10
-5
0
5
10
Velocity (mm/s)